

Measurement of the Branching Fraction $\mathcal{B}(\tau^- \rightarrow h^- \pi^0 \nu_\tau)$

M. Artuso,¹ M. Goldberg,¹ D. He,¹ N. Horwitz,¹ R. Kennett,¹ R. Mountain,¹ G.C. Moneti,¹ F. Muheim,¹ Y. Mukhin,¹ S. Playfer,¹ Y. Rozen,¹ S. Stone,¹ M. Thulasidas,¹ G. Vasseur,¹ X. Xing,¹ G. Zhu,¹ J. Bartelt,² S.E. Csorna,² Z. Egyed,² V. Jain,² K. Kinoshita,³ B. Barish,⁴ M. Chadha,⁴ S. Chan,⁴ D.F. Cowen,⁴ G. Eigen,⁴ J.S. Miller,⁴ C. O'Grady,⁴ J. Urheim,⁴ A.J. Weinstein,⁴ D. Acosta,⁵ M. Athanas,⁵ G. Masek,⁵ H.P. Paar,⁵ M. Sivertz,⁵ J. Gronberg,⁶ R. Kutschke,⁶ S. Menary,⁶ R.J. Morrison,⁶ S. Nakanishi,⁶ H.N. Nelson,⁶ T.K. Nelson,⁶ C. Qiao,⁶ J.D. Richman,⁶ A. Ryd,⁶ H. Tajima,⁶ D. Sperka,⁶ M.S. Witherell,⁶ M. Procario,⁷ R. Balest,⁸ K. Cho,⁸ M. Daoudi,⁸ W.T. Ford,⁸ D.R. Johnson,⁸ K. Lingel,⁸ M. Lohner,⁸ P. Rankin,⁸ J.G. Smith,⁸ J.P. Alexander,⁹ C. Bebek,⁹ K. Berkelman,⁹ K. Bloom,⁹ T.E. Browder,^{9,*} D.G. Cassel,⁹ H.A. Cho,⁹ D.M. Coffman,⁹ D.S. Crowcroft,⁹ P.S. Drell,⁹ R. Ehrlich,⁹ P. Gaidarev,⁹ R.S. Galik,⁹ M. Garcia-Sciveres,⁹ B. Geiser,⁹ B. Gittelman,⁹ S.W. Gray,⁹ D.L. Hartill,⁹ B.K. Heltsley,⁹ C.D. Jones,⁹ S.L. Jones,⁹ J. Kandaswamy,⁹ N. Katayama,⁹ P.C. Kim,⁹ D.L. Kreinick,⁹ G.S. Ludwig,⁹ J. Masui,⁹ J. Mevissen,⁹ N.B. Mistry,⁹ C.R. Ng,⁹ E. Nordberg,⁹ J.R. Patterson,⁹ D. Peterson,⁹ D. Riley,⁹ S. Salman,⁹ M. Sapper,⁹ F. Würthwein,⁹ P. Avery,¹⁰ A. Freyberger,¹⁰ J. Rodriguez,¹⁰ R. Stephens,¹⁰ S. Yang,¹⁰ J. Yelton,¹⁰ D. Cinabro,¹¹ S. Henderson,¹¹ T. Liu,¹¹ M. Saulnier,¹¹ R. Wilson,¹¹ H. Yamamoto,¹¹ T. Bergfeld,¹² B.I. Eisenstein,¹² G. Gollin,¹² B. Ong,¹² M. Palmer,¹² M. Selen,¹² J. J. Thaler,¹² K.W. Edwards,¹³ M. Ogg,¹³ B. Spaan,¹⁴ A. Bellerive,¹⁴ D.I. Britton,¹⁴ E.R.F. Hyatt,¹⁴ D.B. MacFarlane,¹⁴ P.M. Patel,¹⁴ A.J. Sadoff,¹⁵ R. Ammar,¹⁶ S. Ball,¹⁶ P. Baringer,¹⁶ A. Bean,¹⁶ D. Besson,¹⁶ D. Coppage,¹⁶ N. Copty,¹⁶ R. Davis,¹⁶ N. Hancock,¹⁶ M. Kelly,¹⁶ S. Kotov,¹⁶ I. Kravchenko,¹⁶ N. Kwak,¹⁶ H. Lam,¹⁶ Y. Kubota,¹⁷ M. Lattery,¹⁷ M. Momayezi,¹⁷ J.K. Nelson,¹⁷ S. Patton,¹⁷ D. Perticone,¹⁷ R. Poling,¹⁷ V. Savinov,¹⁷ S. Schrenk,¹⁷ R. Wang,¹⁷ M.S. Alam,¹⁸ I.J. Kim,¹⁸ B. Nemati,¹⁸ J.J. O'Neill,¹⁸ H. Severini,¹⁸ C.R. Sun,¹⁸ M.M. Zoeller,¹⁸ G. Crawford,¹⁹ C. M. Daubenmier,¹⁹ R. Fulton,¹⁹ D. Fujino,¹⁹ K.K. Gan,¹⁹ K. Honscheid,¹⁹ H. Kagan,¹⁹ R. Kass,¹⁹ J. Lee,¹⁹ R. Malchow,¹⁹ Y. Skovpen,^{19,†} M. Sung,¹⁹ C. White,¹⁹ F. Butler,²⁰ X. Fu,²⁰ G. Kalbfleisch,²⁰ W.R. Ross,²⁰ P. Skubic,²⁰ M. Wood,²⁰ J. Fast,²¹ R.L. McIlwain,²¹ T. Miao,²¹ D.H. Miller,²¹ M. Modesitt,²¹ D. Payne,²¹ E.I. Shibata,²¹ I.P.J. Shipsey,²¹ P.N. Wang,²¹ M. Battle,²² J. Ernst,²² L. Gibbons,²² Y. Kwon,²² S. Roberts,²² E.H. Thorndike,²² C.H. Wang,²² J. Dominick,²³ M. Lambrecht,²³ S. Sanghera,²³ V. Shelkov,²³ T. Skwarnicki,²³ R. Stroynowski,²³ I. Volobouev,²³ G. Wei,²³ and P. Zadorozhny²³

(CLEO Collaboration)

¹Syracuse University, Syracuse, New York 13244

²Vanderbilt University, Nashville, Tennessee 37235

³Virginia Polytechnic Institute and State University, Blacksburg, Virginia 24061

⁴California Institute of Technology, Pasadena, California 91125

⁵University of California, San Diego, La Jolla, California 92093

⁶University of California, Santa Barbara, California 93106

⁷Carnegie-Mellon University, Pittsburgh, Pennsylvania 15213

⁸University of Colorado, Boulder, Colorado 80309-0390

⁹Cornell University, Ithaca, New York 14853

¹⁰University of Florida, Gainesville, Florida 32611

¹¹Harvard University, Cambridge, Massachusetts 02138

¹²University of Illinois, Champaign-Urbana, Illinois 61801

¹³Carleton University, Ottawa, Ontario, Canada K1S 5B6 and the Institute of Particle Physics, Canada

¹⁴McGill University, Montréal, Québec, Canada H3A 2T8 and the Institute of Particle Physics, Canada

¹⁵Ithaca College, Ithaca, New York 14850

¹⁶University of Kansas, Lawrence, Kansas 66045

¹⁷University of Minnesota, Minneapolis, Minnesota 55455

¹⁸State University of New York at Albany, Albany, New York 12222

¹⁹Ohio State University, Columbus, Ohio 43210

²⁰University of Oklahoma, Norman, Oklahoma 73019

²¹Purdue University, West Lafayette, Indiana 47907

²²University of Rochester, Rochester, New York 14627

²³Southern Methodist University, Dallas, Texas 75275

(Received 1 April 1994)

Using data from the CLEO II detector at the Cornell Electron Storage Ring, we measure $\mathcal{B}(\tau^- \rightarrow h^- \pi^0 \nu_\tau)$ where h^- refers to either π^- or K^- . We use three different methods to measure this branching fraction. The combined result is $\mathcal{B}(\tau^- \rightarrow h^- \pi^0 \nu_\tau) = 0.2587 \pm 0.0012 \pm 0.0042$, in good agreement with standard model predictions.

PACS numbers: 13.35.Dx

The largest decay mode of the tau lepton is to one charged pion, one π^0 , and a neutrino. The branching fraction for this mode is not precisely known, with measured values ranging from 22% to 26% [1,2]. Both the magnitude and shape of the $\pi^- \pi^0$ spectrum provide information on the charged weak spectral function and a test of the conserved vector current (CVC) hypothesis. The significance of the ‘‘one-prong problem’’ [1,3], the gap between the inclusive one-prong branching fraction and the sum of exclusive modes, depends strongly on the magnitude and precision of the $\tau^- \rightarrow h^- \pi^0 \nu_\tau$ branching fraction [4] (referred to as the $h^- \pi^0 \nu_\tau$ mode; h^- refers to either π^- or K^-). In addition, the CLEO measurements of the multi- π^0 ($h^- n \pi^0 \nu_\tau$, $n > 1$) decay branching fractions [5] are normalized to the $h^- \pi^0 \nu_\tau$ mode in order to minimize systematic errors; a precision measurement of the $h^- \pi^0 \nu_\tau$ mode is then needed to turn those ratios into branching fractions.

In this paper we present a precise measurement of the branching fraction $\mathcal{B}_{h\pi^0} \equiv \mathcal{B}(\tau^- \rightarrow h^- \pi^0 \nu_\tau)$. The $h^- \pi^0 \nu_\tau$ mode is dominated by $\rho^- \nu_\tau$, but also receives contributions from $K^* \nu_\tau$, $\rho' \nu_\tau$ and nonresonant $h^- \pi^0 \nu_\tau$ modes. This final state is referred to in this paper as the ρ mode for brevity. No attempt is made to distinguish π^- from K^- in this analysis; the charged particles are assumed to be pions.

Taus are produced in pairs at e^+e^- colliders, and the tau which recoils against the one observed to decay into $h^- \pi^0 \nu_\tau$ is referred to as the tag. We use four different tag decay modes: $e^- \nu_e \nu_\tau$, $\mu^- \nu_\mu \nu_\tau$, $h^- \pi^0 \nu_\tau$, and $h^- h^+ h^- (n \pi^0) \nu_\tau$, denoted as e , μ , ρ , and 3 tag, respectively. We choose combinations of event topologies which yield the branching fraction for $h^- \pi^0 \nu_\tau$ with minimum systematic errors and uncorrelated statistical errors.

Denoting the measured number of background-subtracted, acceptance-corrected events of a given topology by, e.g., $N_{\mu\rho}$ for the μ vs ρ final state, we calculate the branching fraction via the following methods:

$$\mathcal{B}_{h\pi^0} = \sqrt{\frac{N_{e\rho} N_{\mu\rho}}{2N_{e\mu} N_{\tau\tau}}}, \quad \sqrt{\frac{N_{\rho\rho}}{N_{\tau\tau}}}, \quad \text{or} \quad \frac{N_{3-\rho}}{N_{3-1}} \mathcal{B}_1. \quad (1)$$

These will be referred to as the ℓ - ρ , ρ - ρ , and 3- ρ methods, respectively. The ℓ - ρ and ρ - ρ methods normalize to the number of produced tau pairs $N_{\tau\tau}$, determined from the measured luminosity and the theoretical tau pair production cross section, as discussed below; the 3- ρ method is independent of these quantities. Since the branching fraction for the first two methods is determined from the

square root of the measured rates, errors associated with these rates and with $N_{\tau\tau}$ are halved. The ℓ - ρ method arranges the measured rates in a combination that is independent of both the leptonic decay branching fractions of the tau and the lepton identification efficiency. The ρ - ρ method has no dependence on branching fractions other than the one that is being measured. The 3- ρ method is designed to avoid the uncertainty in the three-prong inclusive branching fraction of the tau by normalizing instead to the one-prong inclusive branching fraction \mathcal{B}_1 . The current world average for \mathcal{B}_1 is [1,3] 0.852 ± 0.004 . All three methods depend on understanding the absolute efficiency for reconstructing the π^0 , as well as the level of background from other $\tau^+ \tau^-$ topologies.

The data were accumulated using the CLEO II detector [6] with the Cornell Electron Storage Ring (CESR) e^+e^- collider at beam energy $E_b \sim 5.3$ GeV and center-of-mass energy $E_{c.m.} = 2E_b$. The analysis uses information from a 67-layer tracking system and a 7800-crystal CsI calorimeter, both of which are inside a 1.5 T superconducting solenoidal magnet, and a muon identification system.

A total integrated luminosity of 1.58 fb^{-1} is used for this analysis. The luminosity is measured using $e^+e^- \rightarrow e^+e^-$, $\mu^+\mu^-$, and $\gamma\gamma$ final states, and is determined with an error of 1% [7]. The tau pair production cross section $\sigma(\tau^+\tau^-)$ at these center-of-mass energies is calculated (to order α^3) to be 1.173 times the order α^2 cross section of $86.86/E_{c.m.}^2 \text{ nb}$ ($E_{c.m.}$ in GeV), with a theoretical relative uncertainty of 1% [8]. The total number of produced tau pairs is calculated by summing the cross section times luminosity for each CLEO data run; this yields $N_{\tau\tau} = 1.440 \times 10^6$ produced tau pairs, with a systematic error of 1.4%.

The event selection and π^0 reconstruction methods are similar for all event topologies. For the e - μ , e - ρ , μ - ρ , and ρ - ρ topologies, we require an event to contain exactly two charged tracks separated in angle by $> 90^\circ$. For the 3- ρ and 3-1 topologies, we require an event to contain exactly four charged tracks with three in one hemisphere (as defined by the event thrust axis). The event must have zero net charge.

All charged tracks are required to be observed in the central part of the detector ($|\cos\theta| < 0.71$ where θ is the angle of the track with respect to the e^+ beam), to be consistent with coming from the nominal e^+e^- collision point, and to have momentum greater than $0.1E_b$. Calorimeter showers are considered as candidates for photons from π^0 decays if they are observed in the cen-

tral part of the detector, are not matched to a charged track, and have energy greater than 50 MeV. Pairs of photons with invariant mass within 3.5σ of the π^0 mass (the $\gamma\gamma$ invariant mass rms resolution σ varies from 5 to 10 MeV/ c^2 , depending on π^0 energy) are considered as π^0 candidates. The energy of each π^0 is required to be greater than $0.05E_b$ or $0.10E_b$, depending on the tag. Electrons and positrons are identified by requiring the energy deposited in the calorimeter to be consistent with the momentum of the charged track ($E/p > 0.8$), and the energy deposited in the drift chamber (dE/dx) to be no more than 2σ below that expected for electrons. Muon candidates are required to penetrate ≥ 3 interaction lengths of material in the muon system.

The π^0 candidates are associated with the charged track nearest in angle, to form a $h^-\pi^0$ candidate. The total visible energy in the event must be greater than $0.3E_{c.m.}$, and the net transverse momentum (with respect to the beam line) in the event must exceed $0.075E_b$, to suppress background from two photon processes.

Calorimeter showers that are not matched to charged tracks or used in the ρ candidates can come from several sources, including (a) decays of π^0 's from background $\tau^+\tau^-$ events with higher π^0 multiplicity ("feed-across") or from the hadronic continuum; (b) photons from initial- or final-state or decay radiation; (c) secondary showers from hadronic interactions in the calorimeter, spatially separated from the parent; or (d) showers from detector noise or the circulating beams, but unrelated to the e^+e^- interaction. In order to suppress backgrounds from source (a), we veto events which contain additional showers having energy above 75 MeV, transverse energy profile consistent with that for photons, and >30 cm isolation from the entrance point of any charged track into the calorimeter. In the 3- ρ and 3-1 topologies, extra showers are permitted in the hemisphere containing the 3-prong tag or 1-prong inclusive decay; instead, the invariant mass of all observed particles in these hemispheres is required to be less than the tau mass. Modes containing an unobserved K_L or $\omega \rightarrow \gamma\pi^0$ are considered to be $\tau^+\tau^-$ feed-across, i.e., background for which a correction will be applied. The final branching fraction *does not include* such modes. We assume $\mathcal{B}(\tau^- \rightarrow h^-\pi^0 K_L^0 \nu_\tau) = 0.0035 \pm 0.0018$.

The signal inefficiencies due to sources (b) and (c) (approximately 4% per event and 5% per $h^-\pi^0$, respectively) are estimated using a detailed simulation of the kinematics of signal topologies from the KORALB [8] Monte Carlo event generator, which generates radiative photons from $\tau^+\tau^-$ production and decay, and of the calorimeter response from a GEANT-based [9] detector simulation package. The loss due to source (c) has been carefully checked using independent samples of data containing charged hadrons but no π^0 's. The veto criteria have been designed to be insensitive to the small differences between Monte Carlo and data for hadronic showers, which are more difficult to simulate than electromagnetic showers.

The inefficiency due to source (d) (approximately 1.4%) is simulated by merging random-trigger events from the data with Monte Carlo signal events, and is checked using $e^+e^- \rightarrow \mu^+\mu^-$ events.

The number of events observed in each topology is given in Table I. Also listed is the efficiency for reconstructing the signal topologies (\mathcal{E}_S), estimated from Monte Carlo simulation, and the fraction of observed events from the background (f_B). The backgrounds from $\tau^+\tau^-$ feed-across are estimated using Monte Carlo simulation and world averages [1,3,5] for the branching fractions of the tau to feed-across modes (dominantly from the decay $\tau^- \rightarrow h^-\pi^0\pi^0\nu_\tau$ [5] where one π^0 is not detected).

The efficiencies for reconstruction of signal topologies and tau-pair backgrounds receive contributions from the trigger, charged particle tracking, photon detection, and π^0 reconstruction, and the effect of cuts on momenta, angles, and energies. The trigger efficiency is greater than 99% for all topologies except for e - μ and μ - ρ , where the efficiency is as low as 95% for some data-taking periods. These efficiencies are measured using the data. The charged-track-finding efficiency is also near 100% for the track criteria used here; this is verified by studying independent samples of events with similar topologies. The uncertainty in the track-finding efficiency is 0.5% per track. The lepton identification efficiencies and uncertainties cancel in the ℓ - ρ method [10].

Reconstruction of π^0 decays is well simulated by the GEANT-based Monte Carlo program, as seen in Fig. 1. The peak position, width, low mass tail, and background level are all well reproduced. This is quantified by varying the cuts and methods used to reconstruct photons and π^0 's, and determining the change in the measured branching fraction. Imperfect knowledge of the detector material in front of the calorimeter (and hence the photon conversion rate) also contributes a 0.5% uncertainty to the absolute efficiency for π^0 reconstruction.

The distributions of all kinematical quantities in the signal events are compared between data and Monte Carlo. Examples of such comparisons are shown in Fig. 2. There is good agreement in all distributions, within the accepted region, indicating that the acceptance is well modeled, and that no significant background

TABLE I. For each event topology, we give the total number of events found, the background fraction (f_B), and the signal reconstruction efficiency (\mathcal{E}_S) [10].

Topology	Events	f_B (%)	\mathcal{E}_S (%)
e - ρ	13 353	2.90	9.85
μ - ρ	11 758	2.87	8.89
e - μ	16 088	0.16	17.90
ρ - ρ	6 498	5.87	6.46
3- ρ	12 469	6.69	10.39
3-1	85 959	6.20	22.34

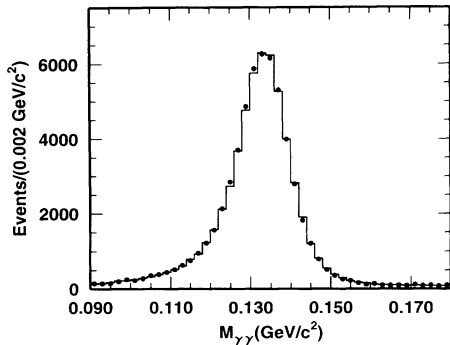


FIG. 1. The $M_{\gamma\gamma}$ distribution for the data (points) and the Monte Carlo simulation (histogram), summed over all tags.

(other than the $\tau^+\tau^-$ feed-across component included in the Monte Carlo simulation) remains in the data. Again, this is quantified by applying new cuts or varying existing ones over a wide range in acceptance, and observing the change in the measured branching fraction. We have performed several other cross checks of our π^0 reconstruction and extra energy veto efficiency using our $\tau^+\tau^-$ data, all of which yield consistent results [11].

The largest source of background in these topologies is from $\tau^+\tau^-$ feed-across events in which the $h^-\pi^0$ system is replaced by a system containing additional π^0 's which are not observed. The sensitivity of our result to uncertainties in these branching fractions [5] is minimized by the tight veto on extra showers; f_B is small (see Table I). Backgrounds from tau decays containing a K_L or ω meson can be estimated reliably from measured branching fractions [1]. Other sources of backgrounds include tau decay modes containing two spurious showers which fake a π^0 ; our π^0 reconstruction algorithms reduce this background to a negligible value. The backgrounds from hadronic continuum and $B\bar{B}$ production are very

TABLE II. Relative systematic errors (%), for the three methods of measuring the branching fraction. The weights from uncorrelated statistical and systematic errors assigned to the three measurements for combining are also given.

Source of error	ℓ - ρ	ρ - ρ	3- ρ
Trigger efficiency	0.7	0.2	0.1
Tracking efficiency	0.5	0.5	0.2
π^0 reconstruction	0.9	0.9	0.9
Acceptance	0.5	0.5	1.1
Extra shower veto	0.9	0.9	0.9
MC statistics	0.5	0.4	0.6
$\tau^+\tau^-$ feed-across	0.3	0.4	0.7
Non- τ backgrounds	0.2	0.4	0.4
Luminosity	0.5	0.5	...
$\sigma(\tau^+\tau^-)$	0.5	0.5	...
\mathcal{B}_1	0.4
Combined	1.9	1.8	2.0
Weight (%)	27	45	28

small except in the 3- ρ and 3-1 topologies; they are estimated from the data, using events in which the invariant mass of all observed particles in the 3-prong hemisphere is greater than the tau mass [12].

The systematic errors associated with uncertainties in the signal efficiency (\mathcal{E}_S), the background fraction (f_B), and the number of produced tau pairs ($N_{\tau\tau}$), are tabulated for the three methods in Table II. The largest sources of uncertainty are the absolute π^0 reconstruction efficiency, the inefficiency due to the extra shower veto,

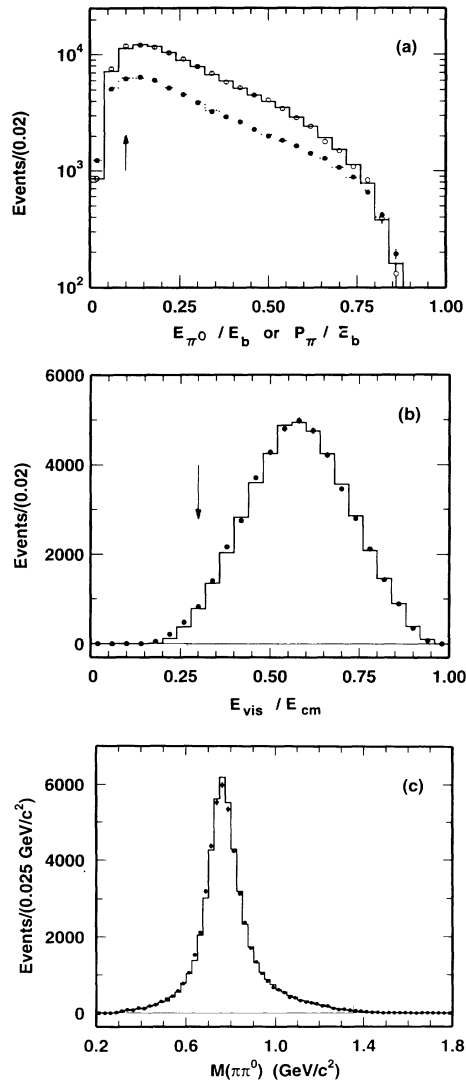


FIG. 2. The distributions of a variety of kinematical variables for the data (points) and the Monte Carlo simulation (histogram), summed over all tags. (a) The scaled momentum of the charged particles, p_π/E_b (open circles and solid histogram), and the scaled energy of the π^0 , E_{π^0}/E_b (solid circles and dotted histogram, scaled by a factor 3 for clarity); (b) the scaled visible energy, $E_{\text{vis}}/E_{\text{c.m.}}$; (c) the $\pi^-\pi^0$ invariant mass. The accepted region is to the right of the vertical arrows in (a) and (b).

and the modeling of the inclusive 3-prong decay acceptance. Many of the largest sources of systematic errors (in particular, the π^0 reconstruction and extra shower veto efficiencies) are common to all three methods, and the ℓ - ρ and ρ - ρ methods share the errors in tracking efficiency, luminosity, and $\sigma(\tau^+\tau^-)$.

The values of $\mathcal{B}_{h\pi^0}$ determined using Eq. (1) are

$$\begin{aligned} \mathcal{B}_{h\pi^0} &= 0.2559 \pm 0.0019 \pm 0.0047 & (\ell\text{-}\rho), \\ \mathcal{B}_{h\pi^0} &= 0.2567 \pm 0.0017 \pm 0.0045 & (\rho\text{-}\rho), \\ \mathcal{B}_{h\pi^0} &= 0.2643 \pm 0.0029 \pm 0.0052 & (3\text{-}\rho), \\ \mathcal{B}_{h\pi^0} &= 0.2587 \pm 0.0012 \pm 0.0042 & (\text{combined}). \end{aligned} \quad (2)$$

The combined result is obtained by weighting each measurement's statistical and uncorrelated systematic errors; these weights are given in Table II. The three measurements have a χ^2 of 2.4 for 2 degrees of freedom.

The $K^-\pi^0\nu_\tau$ component of our signal is obtained from an independent measurement [13] of the branching fraction $\mathcal{B}(\tau^- \rightarrow K^-\pi^0\nu_\tau) = 0.0051 \pm 0.0011$. Thus, the $\pi^-\pi^0\nu_\tau$ mode branching fraction is $\mathcal{B}_{\pi\pi^0} = 0.2536 \pm 0.0044$. This compares well with a prediction [14] derived from CVC and data on the cross section $\sigma(e^+e^- \rightarrow \pi^+\pi^-)$, $\mathcal{B}_{\pi\pi^0} = 0.2458 \pm 0.0093 \pm 0.0027 \pm 0.0050$, where the errors are from the e^+e^- data, the tau lifetime, and radiative corrections, respectively.

In conclusion, we have presented a high-precision measurement of the branching fraction for the decay $\tau^- \rightarrow h^-\pi^0\nu_\tau$. We have employed four tagging decays, in three statistically independent combinations, which are in good agreement with each another. Common systematic errors limit the overall precision to $\sim 1.7\%$ [11].

The measured value is larger and more precise than previous measurements [1,2]. This value, in combination with resulting larger multi- π^0 ($h^-n\pi^0\nu_\tau$) branching fractions [5], reduces the magnitude and significance of the one-prong problem.

We gratefully acknowledge the effort of the CESR staff in providing us with excellent luminosity and running conditions. This work was supported by the National Science Foundation, the U.S. Department of Energy, the Heisenberg Foundation, the SSC Fellowship program of

TNRLC, and the A.P. Sloan Foundation.

* Permanent address: University of Hawaii at Manoa, Honolulu, HI 96822.

† Permanent address: INP, Novosibirsk, Russia.

- [1] K. Hikasa *et al.*, Phys. Rev. D **45**, 1 (1992). See also the 1994 "Review of Particle Properties" (to be published).
- [2] Recent and preliminary results from DELPHI, OPAL, ARGUS, and ALEPH were presented by A. Schwarz, in *The Proceedings of the XVI International Symposium on Lepton Photon Interactions, Cornell University, August 1993*, edited P. Drell and D. Rubin (AIP, New York, 1994).
- [3] See, for example, A. Weinstein and R. Stroynowski, Annu. Rev. Nucl. Part. Sci. **43**, 457 (1993). We assume that the one-prong branching fraction \mathcal{B}_1 excludes modes containing $K_S \rightarrow \pi^+\pi^-$ decays; the systematic error on \mathcal{B}_1 is increased to account for this ambiguity.
- [4] In this Letter, charge conjugate states are implied.
- [5] M. Procario *et al.*, Phys. Rev. Lett. **70**, 1207 (1993).
- [6] Y. Kubota *et al.*, Nucl. Instrum. Methods Phys. Res., Sect. A **320**, 66 (1992).
- [7] G. Crawford *et al.*, Report No. CLNS 94/1268, 1994 (to be published).
- [8] KORALB (v.2.1) / TAUOLA (v.1.5): S. Jadach and Z. Was, Comput. Phys. Commun. **36**, 191 (1985); **64**, 267 (1991); S. Jadach, J.H. Kühn, and Z. Was, Comput. Phys. Commun. **64**, 275 (1991); **70**, 69 (1992); **76**, 361 (1993).
- [9] R. Brun *et al.*, GEANT 3.15, CERN DD/EE/84-1.
- [10] These uncertainties are not negligible, and precision measurements of leptonic or three-prong inclusive branching fractions cannot be obtained from the yields in Table I.
- [11] Further details on the systematic errors, and studies of the $\pi^-\pi^0$ invariant mass and decay angle distributions, will be presented in a future publication.
- [12] The method is described in D. Bortoletto *et al.*, Phys. Rev. Lett. **71**, 1791 (1993).
- [13] M. Battle *et al.*, Report No. CLNS 94/1273, 1994 (to be published).
- [14] J. Kühn and A. Santamaria, Z. Phys. C **48**, 443 (1990); W. Marciano, in *Proceedings of the Second Workshop on Tau Lepton Physics, September 1992*, edited K.K. Gan (World Scientific, Singapore, 1993).